J. Water Environ. Nanotechnol., 4(2): 167-173 Spring 2019

ORIGINAL RESEARCH PAPER

Calculation Study of Conversion Nitrate Ions to N_2 and O_2 by Zinc Oxide Nano-Cage ($Zn_{12}O_{12}$-NC)

Leila Mahdavian

Department of Chemistry, Doroud Branch, Islamic Azad University, Doroud. Iran

Received: 2019-01-28 Accepted: 2019-04-12 Published: 2019-05-01

ABSTRACT

The aim of this study is to investigate the performance of zinc oxide nano-cages ($Zn_{12}O_{12}$-NC) to detect and reduce nitrate (NO^{3-}) ions from aqueous media and convert them to oxygen and nitrogen gases by the density functional theory (DFT) method on a B3LYP level with basis set of 6-31+G*. Due to the structure of the nano-cage ($Zn_{12}O_{12}$-NC), there are some location positions with different potential on it. The results showed that the first N atom of nitrate ion strongly prefers to be adsorbed on O atoms and O of nitrate ion is adsorbed on Zn atoms of the 4-membered ring (4-MR). The *electronic*, structure and thermodynamic properties of these conversions are calculated and investigated. The energy gap (E_g) of the $Zn_{12}O_{12}$-NC is dramatically reduced from 3.88 to 1.22 eV upon the adsorption of NO^{3-} ion, suggesting that it is transformed to n-type semiconductor ascribed to the large charge transfer from the ion to the nano-cage and ions convert into oxygen and nitrogen on it. The data show that $Zn_{12}O_{12}$ nano-cage can be used to identify and reduce nitrate ions from the environment and may be helpful in several fields of study such as sensors, catalysts, and field emission investigations.

Keywords: *DFT Method, Nano-Sensor, Nitrate Ions, Thermodynamic Properties, Zn12O12 Nano-Cage*

How to cite this article

Mahdavian L. Calculation Study of Conversion Nitrate Ions to N_2 and O_2 by Zinc Oxide Nano-Cage ($Zn_{12}O_{12}$-NC). J. Water Environ. Nanotechnol., 2019; 4(2): 167-173. DOI: 10.22090/jwent.2019.02.008

INTRODUCTION

The nitrate ion is considered as a serious threat to the environment and aquatic ecosystems as one of the main sources of pollution [1]. There are several methods to remove nitrate ions from drinking water. The diluted, ion exchange and reverse osmosis are the most common methods for large-scale nitrate reduction [2]. Nowadays, nanotechnology has attracted the attention of researchers because of its low cost and high efficiency in removing pollutants [3]. The nanoparticles have a high ratio of surface to the volume which increases the reactivity of nanoparticles, therefore, have high sensitivity and fast response time to pollutants [4]. Thus, the development of nano-sensors for identification and reduction of these pollutants is the most important.

The nano-sensors of C_n nanocage [5], graphene [6], $Ca_{12}O_{12}$ nanocages [7], ZnO nanotube [8], $X_{12}Y_{12}$ (X=Al, B and Y=N, P) nanocluster [9, 10], $B_{12}N_{12}$ nano-cage [11] and so on are used for detection of pollutants and toxic ions. $X_{12}Y_{12}$ nano-cage is magic and is more stable, this nano-cage is formed from six 4-membered rings (4-MRs) and eight 6-membered rings (6-MRs) with T_h symmetry (The optimized structure of $Zn_{12}O_{12}$ nano-cage is in Fig. 1).

Zinc oxide is one of the available compounds which can be used to remove pollutants [12, 13], is known as a safe substance [14] and is one of the best options for removal of nitrate ion from the environment. A significant characteristic of zinc oxide is: piezoelectric, semiconductors, being inexpensive, bring non-toxic, bring abundant in nature, being environmentally friendly, having high thermal stability and so on [15-18]. Zinc nano-oxide sorbents have various structures,

* Corresponding Author Email: *mahdavian@iau-doroud.ac.ir*

depends on the process of synthesis. They may be zinc oxide nanoparticles (Wurtzite) [19], nanospheres [20], nano boxes [21], hexagonal, tripods [22], tetrapods [23], nanowires, nanotubes, nanorings [24–27], nanocages, and nanoflowers [28, 27]. The Zn-O atoms are a bond of polarity because of a positive charge at Zn and a negative charge at O atom positions; can be an electrophilic or nucleophile molecule. The $Zn_{12}O_{12}$ nano-cage has been extensively studied at a theoretical level in compared to other its forms. The capacity of the $Zn_{12}O_{12}$ to adsorption different chemical species has been investigated: NO [28], H_2S [29], Cl_2 [12] and so on.

In this study, for the removal and reduction of nitrate ions from aqueous solution is used zinc oxide nano-cage ($Zn_{12}O_{12}$-NC). The interaction of nitrate ions with $Zn_{12}O_{12}$ nano-cage will be theoretically investigated based on analyses of structure, energies, HOMO-LUMO gaps (E_g), stability, electrical and thermodynamic properties and so on. Our results are likely to be useful for further studies related to making of $Zn_{12}O_{12}$ nano-cage ($Zn_{12}O_{12}$-NC): as nano-sensor, for investigation of this interaction is used GAMESS-US [30] of the program package in windows.

COMPUTATIONAL METHOD

Computational chemistry includes various mathematical methods which are divided into two groups: 1-molecular mechanics, 2-quantum mechanics. One of the most public computational programs is the quantum chemistry of Gaussian, which is developed by a Sir John Anthony Pople group in Peterborough [31]. Computations can be done on the systems in the gas phase or in the solution, and in the state of base or stimulating. The GAMESS-US program package used a wide range of Density Function theory models and energies decompose ingredients, decompose frequencies computed for all DFT models [32, 33]. All states of similarity of nitrate ion to zinc oxide nano-cage are optimized by B3LYP/6-31+G*. To study the thermodynamic properties, electrical and so on are calculated by this method for stages of conversion NO_3^- to N_2 and O_2 As follows:

$$2NO_3^- + ZnO\text{-}NC \leftrightarrow 2NO_3^-ZnO\text{-}NC$$
$$2NO_3^-ZnO\text{-}NC \leftrightarrow N_2 + 3O_2 + ZnO\text{-}NC$$

Energy and optimized geometric structure of molecules have a concrete relationship with chemical phenomena and the amounts of other similar atomic loads and border orbitals are less determined by qualitative results. Basically, the catalytic properties of the compositions are totally determined by their electronic structure. Therefore, designing the electronic structure based on the change in composition and physical structure is important. After simulation of $Zn_{12}O_{12}$-NC structure [34], is optimized by B3LYP/6-31+G* which can be observed in Fig. 1. The $Zn_{12}O_{12}$ nano-cage includes eight hexagonal rings (6-MRs) and six four-membered rings (4-MRs), Zinc and oxygen atoms have been equally and alternately placed inside the ring with T_h symmetry. The heat of formation, geometric form of the molecule, ionization energy, electronic and other properties are calculated for nano-cage and NO_3^- ion, separately and then converted NO_3^- ions to N_2 and O_2 on nano-cage. The binding energy (E_{bin}) of NO_3^- ions on the nano-cage has been obtained using the following equation:

$$E_{bin} = E_{X\text{-}ZnO\text{-}NC} - [E_X + E_{ZnO\text{-}NC}] + \delta_{BSSE} \quad (1)$$

In this equation, the $E_{X\text{-}ZnO\text{-}NC}$ is the total energy of pollutant energy (X) and (nano-adsorbent is

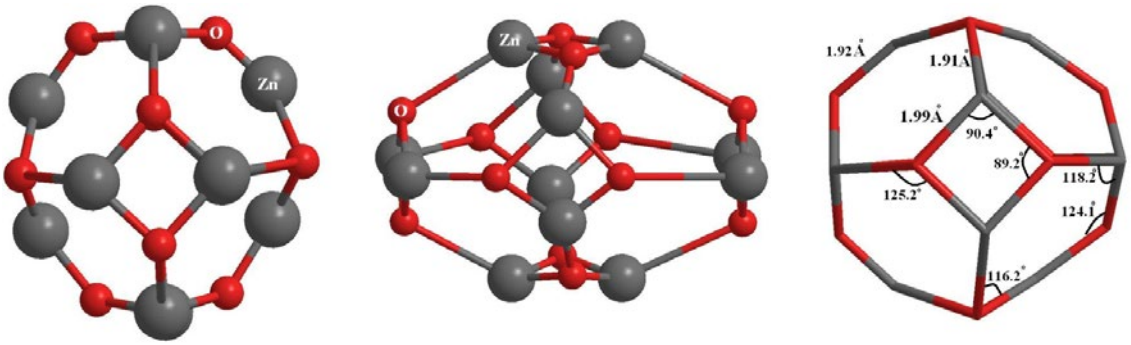

Fig. 1. Ball and stick model of the optimized geometric structure of $Zn_{12}O_{12}$-NC from different views.

subtracted from the pollutant complex energy with zinc oxide nano-cage ($Zn_{12}O_{12}$-NC) until the amount of change of thermodynamic and structural parameters of the reaction is achieved in which δ_{BSSE} is the amount of computational mistake.

RESULTS AND DISCUSSION

The accomplished computations for achieving structural properties are based on B3LYP/6-31+G* method which was performed at 298K temperature in an aqueous medium. In order to study the reaction of nitrate ion with nano-adsorbent for computing thermodynamic parameters, first the computational data from nano-cage and also nitrate ion are computed separately as shown in Table 1. The computed thermodynamic and structural properties of these structures by use of B3LYP/6-31+G* method are: the total energy (E_{total}), dipole moment (DM), the root mean square (RMS), the binding energy (E_{bin}), the heat of formation (H), the Gibbs free energy (G_{ele}), the nuclear energy (E_{nuc}) and electric energy (E_{ele}).

The obtained results show that greater structural symmetry leads to lower structural dipole moment and less polarity. The zinc oxide nano-cage is more symmetrical and also has a less RMS gradient. The zinc oxide nanocage is used, has twelve zinc and oxygen atoms which can also be shown in the form of $Zn_{12}O_{12}$-NC. Development of nano-cage compounds has caused extreme progress in the sciences, that it is called magical mixes.

As it can be observed in Fig. 2, there are several places for the interaction between pollutant and nano-cage. This nano-adsorbent has been made of two series of 6-RMs ring and 4-RMs ring which have different field and spatial positions to absorb pollutant. These positions are shown in Fig. 2. The nitrate ion can be close to one of these four positions. All probabilities are simulated.

Table 2 shows the computational parameters of all probabilities. Among all positions, first and fourth positions have a high dipole moment in compared to other positions, but thermodynamic

Table 1. The structural and thermodynamic parameters of nitrate and zinc oxide nano-cages at 298K.

Nano-absorber	E_{total} kcal/mol	*Dipole Moment* (D)	*RMS* kcal/ml. Å	E_{bin} kcal/mol	*H* kcal/mol	G_{ele} kcal/mol	E_{nuc} kcal/mol	E_{elec} (kV)
NO_3^-	-27176.2	3.418	125.5	-239.17	104.61	-61904	34727.77	0.0003
$Zn_{12}O_{12}$-NC	-129957.6	0.62	641.1	1903.66	2930.07	-609651.8	479694.2	0.0032

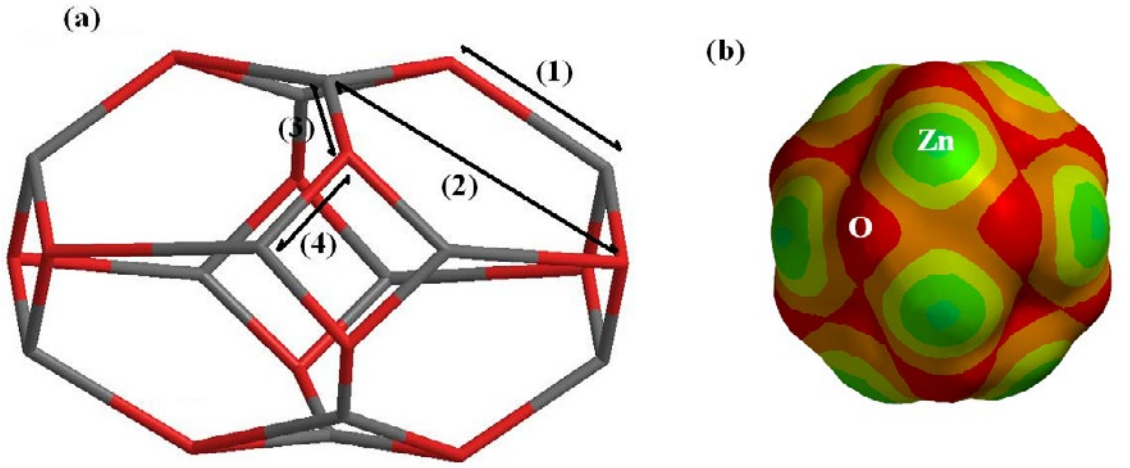

Fig. 2. a) the different positions of closed nitrate ion to $Zn_{12}O_{12}$ nano-cage and b) the molecular electrostatic potential surface $Zn_{12}O_{12}$ nano-cage.

Table 2. The structural and thermodynamic properties of closed nitrate ions to different positions of zinc oxide nano-cage at 298K.

Steps	E_{total} kcal/mol	*Dipole Moment* (D)	*RMS* kcal/ml. Å	E_{bin} kcal/mol	*H* kcal/mol	G_{ele} kcal/mol	E_{nuc} kcal/mol	E_{elec} (kV)
1	-11252.3	11.62	615.8	-64.08	-64.08	394262.0	-282047.1	-0.0021
2	-10668.5	5.67	770.3	-319.73	-221.17	330575.2	-255132.0	-0.0017
3	-11452.5	6.69	593.4	-264.25	-354.08	315405.1	-252351.3	-0.0016
4	-11592.0	7.03	599.3	-403.85	-403.86	-217661.0	206369.2	0.0011

properties calculated for the fourth position show a significant difference compared to other positions, that electrical energy (E_{ele}) of this position is much more than other positions in a way that it is 0.0011 kV. The G_{ele} (kcal.mol^{-1}) and H (kcal.mol^{-1}) calculated for the 4th position are at their lowest and the total energy for this position is lower. Thus, the possibility of closed nitrate ion to the 4th position of $Zn_{12}O_{12}$-NC is more than other positions.

In $Zn_{12}O_{12}$-nanocage, Zn atoms are positively charged (green colors) while the O atoms are negatively charged (red colors) in Zn-O bond, indicating the ionic character of these bonds by the molecular electrostatic potential surface in Fig. 2.

So, the closed nitrate ions to the fourth position on zinc oxide nano-cage are simulated in three stages. In Fig. 3, the D stage is a step close pollutants to $Zn_{12}O_{12}$-nanocage, the TS`$_1$ is the transition state of the complex formed between pollutants and $Zn_{12}O_{12}$-NC that occurred exchanging electrons between them and goes into produces and E stage is the formation of produces (N_2 and O_2 molecules).

After adsorption of nitrate ions and the exchange of electrons between them, they are transformed into gaseous molecules of nitrogen and oxygen. The proposed mechanism after absorption of nitrate ions on $Zn_{12}O_{12}$-NC is as follows:

$$NO_3^- + NO_3^- \leftrightarrow 2NO_2 + O_2 + 2e^-$$
$$2NO_2 \leftrightarrow 2NO + O_2$$
$$2NO \leftrightarrow N_2 + O_2$$

Computed data of these stages can be observed in Table 3 and the greatest changes in the structure and thermodynamic changes are in the transition state TS`$_1$. The E_{ele} for this stage has most changes, is 3.2 V. Because of the symmetry structure of NO_3^- ions changes from T_h to $D_{\infty h}$ and the polarity of $Zn_{12}O_{12}$ nano-cage increases.

As it can be seen in obtaining computational data in Tables 3 and 4, the center of zinc oxide nano-cage is the most sensitive position for adsorption of pollutants. Thus, the Gibbs free energy (ΔG_{ele}), the heat of formation (ΔH), entropy (ΔS_{ele}) and the equilibrium constant (K) is calculated between 1st and 2nd steps. The data of Table 4 show that this reaction is spontaneous. The entropy change (ΔS_{ele}) is positive; it is of the entropy increase type. Considering the changes in thermodynamic functions, the reaction is favorable because of the negative Gibbs free energy (ΔG_{ele}), and the positive entropy change (ΔS_{ele}). Therefore, $Zn_{12}O_{12}$-nanocage can be used as a sensor for the measurement and reduction of nitrate ions from the environment.

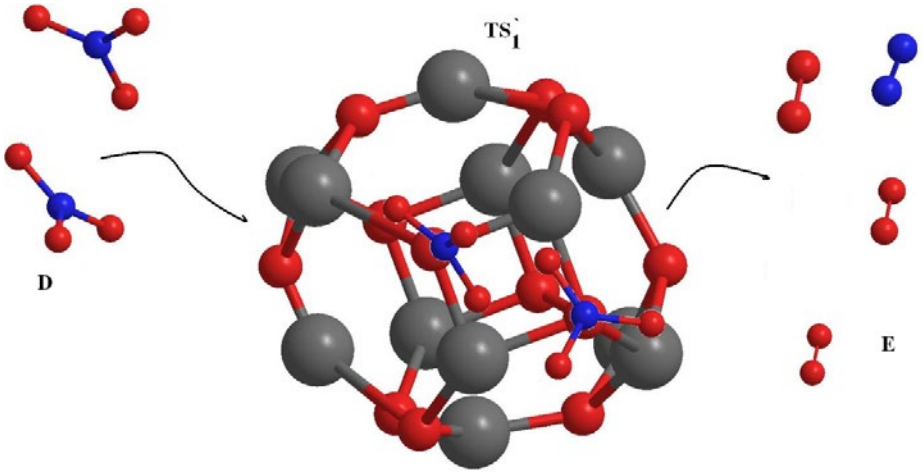

Fig. 3. The pathway of interaction and the electron transport of nitrate ions with the adsorbent of $Zn_{12}O_{12}$ nano-cage.

Table 3. The calculation of electrical energy (E_{elec}), Dipole Moment (DM), RMS gradient, total energy (E_{total}), heat of reaction formation (H), Gibbs free energy (G_{ele}), nucleus energy (E_{nuc}) and binding energy (E_{bin}) for D, TS`$_1$ and E by B3LYP/6-31+G* method at 298K.

Steps	E_{total} kcal/mol	*Dipole Moment* (D)	*RMS* kcal/ml. Å	E_{bin} kcal/mol	*H* kcal/mol	G_{ele} kcal/mol	E_{nuc} kcal/mol	E_{elec} (V)
D	-50591	10.01	571.5	-1277.68	-3098.76	-572910	-796469	2.9
TS`$_1$	-35151.9	557.4	2427	14161.44	14505.21	-611808	-769554	3.2
E	199614	938.5	4406	261152.1	261617.7	-150551	-766773	0.8

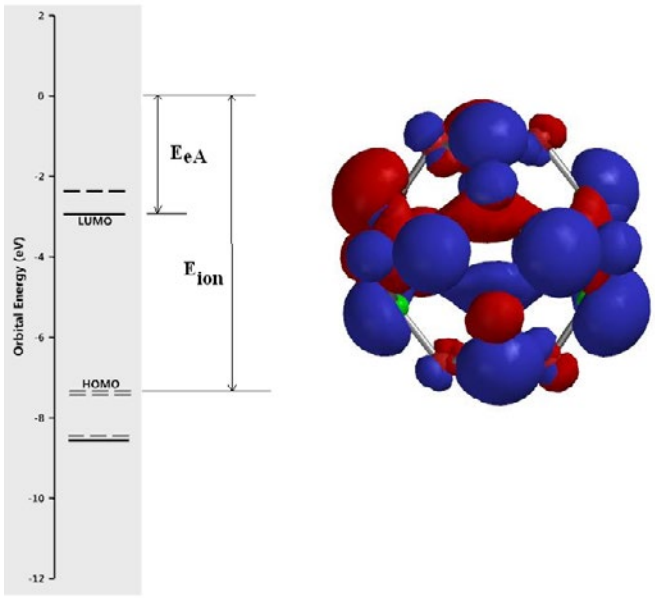

Fig. 4. Differences in the energy levels of LUMO and HOMO with the hardness and softness of the $Zn_{12}O_{12}$-NC.

Table 4. The thermodynamic parameters of conversion nitrate ions to N_2 and O_2 on $Zn_{12}O_{12}$-nanocage.

Nano-absorber	ΔG_{ele} kcal/mol	ΔH kcal/mol	ΔS_{ele} kcal/K.mol	K
NO_3^--$Zn_{12}O_{12}$nanocage	-38898	17603.97	189.60	65940.2

Table 5. DOS calculations for the NO_3^- ion and the nano-adsorbents optimized by the B3LYP/6-31+G* computational method.

	E_{LUMO}/eV	E_{HOMO}/eV	E_g/eV	η /eV	μ /eV	σ/eV	ω/eV	ΔN_{MAX}/eV
$Zn_{12}O_{12}$-NC	-3.66	-7.54	3.88	-5.6	1.94	-0.94	8.08	2.89
D	-1.10	-5.31	4.21	-3.21	2.11	-1.11	2.44	1.52
TS`$_1$	-1.25	-2.47	1.22	-1.86	0.61	0.39	2.84	3.05
E	-2.34	-6.28	3.94	-4.31	1.97	-0.97	4.71	2.19

The structural parameters can be achieved based on the energy levels of the lowest unoccupied molecular orbit (LUMO) and the highest occupied molecular orbit (HOMO). The electron-affinity energy of the molecule is a baseline difference with the energy level of LUMO, and the ionization energy of the molecule is the difference in the baseline energy level with the energy level of HOMO. The total energy of the two levels is twice the electronegativity (η) of the molecule, which is a criterion for the hardness and softness of the molecular structure (Fig. 4).

The molecule will have a smooth structure and a high polarization when the two energy levels (above) are close to each other. If the two energy levels are higher distant, the molecule structure will be harder with a lower polarization. The energy difference between the two levels is called the energy gap (E_g), which represents the conductivity level of the molecular structure. The chemical potential or electronegativity (η) [the E_{eA} and E_{ion} are electron affinity and ionization energy, respectively], chemical hardness (μ), chemical softness (σ), electrophilicity (ω), and molecular charge transfer (ΔN_{MAX}) were calculated using the following relationships:

$$E_g = E_{LUMO} - E_{HOMO} \quad (2)$$

$$\eta = (E_{LUMO} + E_{HOMO})/2 \quad (3)$$

$$\mu = (E_{LUMO} - E_{HOMO})/2 \quad (4)$$

$$\sigma = 1 - \mu \quad (5)$$

$$\omega = \eta^2/2\,\mu \quad (6)$$

$$\Delta N_{MAX} = -\eta / \mu \quad (7)$$

The calculated parameters (Table 5) show that

the orbital gap energy (E_g) is very important to control and detect sensors and filters. The lower the amount of E_g, the greater the nano-adsorbent conductivity; in other words, the transmission of electrons between the nitrate ions and the nano-adsorbent increases when the distance between the HOMO and LUMO energy levels is lower in order to generate an electrical signal. The relationship between the electric conductivity (E_c) and the orbital gap energy (E_g) is shown below:

$$E_c \propto \exp(-E_g/2kT) \quad (8)$$

where k is the Boltzmann constant and T is the ambient temperature. This equation shows a direct relationship between E_c and E_g, indicating a better electrical conductivity for $Zn_{12}O_{12}$-NC when ions are close to it.

According to the data in Table 5, The E_g decreases for the $TS`_1$ stage, therefore $Zn_{12}O_{12}$-NC is an n-type semiconductor. The μ and σ denote the hardness and softness of the molecules, respectively. HOMOs and LUMOs in hard and soft molecules have large and low gaps, respectively. The molecular charge transfer (ΔN_{MAX}) reflects the electron donority or receivability of the pollutant and the nano-adsorbents.

CONCLUSION

The zinc oxide nanocage was used in this study to remove nitrate ions from the water environment. All of the structures of $Zn_{12}O_{12}$-nanocage and pollutant have been optimized using DFT methods by B3LYP/6-31+G*. The structural and thermodynamic properties of these interactions have been calculated by this method and the reason for choosing this computational method are computation speed, obtaining electrical properties and so on. Due to Zn metal using in nano-cage finds this based set of the calculations. The Nano-cage interaction with nitrate ions is in the center position of the $Zn_{12}O_{12}$-NC and the exchange of electrons between them is better in this position. The results of the thermodynamic show that the conversion of nitrate ions to nitrogen and oxygen molecules on the $Zn_{12}O_{12}$-nanocage is possible. The $Zn_{12}O_{12}$-NC has semiconducting properties with direct energy gap and is particularly stable at room temperature. The nitrate ions are all chemisorbed on the $Zn_{12}O_{12}$-NC with reasonable adsorption energies. The electronic properties of the $Zn_{12}O_{12}$-NC present dramatic changes after the adsorption of the nitrate ions, especially their electric conductivity. Therefore, synthetically considering the adsorption energies, charge transfer and the change of electric conductivity can conclude that the $Zn_{12}O_{12}$-NC is a potential candidate for nanosensors with high sensitivity for nitrate ions.

CONFLICT OF INTEREST

The authors declare that there are no conflicts of interest regarding the publication of this manuscript.

REFERENCES

1. Samatya S, Kabay N, Yüksel Ü, Arda M, Yüksel M. Removal of nitrate from aqueous solution by nitrate selective ion exchange resins. Reactive and Functional Polymers. 2006;66(11):1206-14.
2. M. Matošić, I. Mijatović and E.Hodžić. Nitrate Removal from Drinking Water Using Ion Exchange – Comparison of Chloride and Bicarbonate form of the Resins. Chem. Biochem. Eng. Q. 14(4) (2000)141-146.
3. Liu H, Guo M, Zhang Y. Nitrate removal by Fe0/Pd/Cu nano-composite in groundwater. Environmental Technology. 2013;35(7):917-24.
4. Kim Y-J, Choi J-H. Selective removal of nitrate ion using a novel composite carbon electrode in capacitive deionization. Water Research. 2012;46(18):6033-9.
5. Qin H, Huang Y, Liu S, Fang Y, Li X, Kang S. Synthesis and Properties of Magnetic Carbon Nanocages Particles for Dye Removal. Journal of Nanomaterials. 2015;2015:1-8.
6. Hosseini M, Ghozatloo A, Shariaty-Niassar M. Effect of CVD graphene on hydrate formation of natural gas. Journal of Nanostructure in Chemistry. 2015;5(2):219-26.
7. Rad AS, Aghaei SM, Pazoki H, Binaeian E, Mirzaei M. Surface interaction of H2 O and H2 S onto Ca12 O12 nanocluster: Quantum-chemical analyses. Surface and Interface Analysis. 2018;50(4):411-9.
8. Soheili HN, Mahdavian L. Reduction and Conversion of Nitrate Ions from the Environment by Zinc Oxide Nano-Sensor (ZnO-NS): IR and NMR-Density Functional Theory Study. Sensor Letters. 2017;15(6):469-74.
9. Rad AS, Ayub K. DFT study of boron trichloride adsorption on the surface of Al12N12 nanocluster. Molecular Physics. 2017;115(7):879-84.
10. Rad AS. Comparison of X12Y12 (X=Al, B and Y=N, P) fullerene-like nanoclusters toward adsorption of dimethyl ether. Journal of Theoretical and Computational Chemistry. 2018;17(02):1850013.
11. Mahdavian L. Study of Reduction 2,3,7,8-Tetrachlorodibenzodioxine by B12N12 Nano-Cage: NMR and NBO-DFT. Materials Focus. 2016;5(5):458-63.
12. Baei MT, Peyghan AA, Bagheri Z. Quantum chemical analysis on hydrogenated Zn12O12 nanoclusters. Comptes Rendus Chimie. 2013;16(2):122-8.
13. Beheshtian J, Peyghan AA, Bagheri Z. Adsorption and dissociation of Cl2 molecule on ZnO nanocluster. Applied Surface Science. 2012;258(20):8171-6.
14. Bagabas A, Alshammari A, Aboud MFA, Kosslick H. Room-temperature synthesis of zinc oxide nanoparticles

in different media and their application in cyanide photodegradation. Nanoscale Research Letters. 2013;8(1).
15. Pourrahimi AM, Liu D, Pallon LKH, Andersson RL, Martínez Abad A, Lagarón JM, et al. Water-based synthesis and cleaning methods for high purity ZnO nanoparticles – comparing acetate, chloride, sulphate and nitrate zinc salt precursors. RSC Adv. 2014;4(67):35568-77.
16. Luo Z, Zhu S, Liu Z, Liu J, Huo M, Yang W. Study of phosphate removal from aqueous solution by zinc oxide. Journal of Water and Health. 2015;13(3):704-13.
[17] A. Fallah Shojaei, F. Golriz. High photocatalytic activity in nitrate reduction by using Pt/ZnO nanoparticles in the presence of formic acid as hole scavenger. Bulg. Chem. Commun. 47(2) (2015) 509-514.
18. Bhatnagar A, Ji M, Choi YH, Jung W, Lee SH, Kim SJ, et al. Removal of Nitrate from Water by Adsorption onto Zinc Chloride Treated Activated Carbon. Separation Science and Technology. 2008;43(4):886-907.
19. Siddiqi KS, ur Rahman A, Tajuddin, Husen A. Properties of Zinc Oxide Nanoparticles and Their Activity Against Microbes. Nanoscale Research Letters. 2018;13(1).
20. Kakiuchi K, Hosono E, Kimura T, Imai H, Fujihara S. Fabrication of mesoporous ZnO nanosheets from precursor templates grown in aqueous solutions. Journal of Sol-Gel Science and Technology. 2006;39(1):63-72.
21. Mahmud S, Abdullah MJ. Nanotripods of Zinc Oxide. 2006 IEEE Conference on Emerging Technologies - Nanoelectronics: IEEE.
22. Shen L, Zhang H, Guo S. Control on the morphologies of tetrapod ZnO nanocrystals. Materials Chemistry and Physics. 2009;114(2-3):580-3.
23. Ding Y, Wang ZL. Structures of planar defects in ZnO nanobelts and nanowires. Micron. 2009;40(3):335-42.
24. Wang ZL. Nanostructures of zinc oxide. Materials Today. 2004;7(6):26-33.
25. Wang ZL. Zinc oxide nanostructures: growth, properties and applications. Journal of Physics: Condensed Matter. 2004;16(25):R829-R58.
26. Moezzi A, Cortie M, McDonagh A. Aqueous pathways for the formation of zinc oxide nanoparticles. Dalton Transactions. 2011;40(18):4871.
27. Xie J, Li P, Li Y, Wang Y, Wei Y. Morphology control of ZnO particles via aqueous solution route at low temperature. Materials Chemistry and Physics. 2009;114(2-3):943-7.
28. Peyghan AA, Noei M. Electronic Response of Nano-sized Cages of ZnO and MgO to Presence of Nitric Oxide. Chinese Journal of Chemical Physics. 2013;26(2):231-6.
29. Peyghan AA, Baei MT, Hashemian S. ZnO Nanocluster as a Potential Catalyst for Dissociation of H2S Molecule. Journal of Cluster Science. 2013;24(1):341-7.
[30] R. Ahmadi, M. Pirahan-Foroush, Ab initio studies of fullerene effect on chemical properties of naphazoline drop. AMHSR. 12 (2014) 86-90.
31. Becke AD. Density-functional thermochemistry. III. The role of exact exchange. The Journal of Chemical Physics. 1993;98(7):5648-52.
32. Metropolis N, Rosenbluth AW, Rosenbluth MN, Teller AH, Teller E. Equation of state calculations by fast computing machines. Office of Scientific and Technical Information (OSTI), 1953 1953/03/06. Report No.
33. Wang L, Huang X, Xia J, Zhu D, Li X, Meng X. Three dimensional ZnO nanotube arrays and their optical tuning through formation of type-II heterostructures. CrystEngComm. 2016;18(14):2517-23.
34. de Oliveira OV, Pires JM, Neto AC, Divino dos Santos J. Computational studies of the Ca12O12, Ti12O12, Fe12O12 and Zn12O12 nanocage clusters. Chemical Physics Letters. 2015;634:25-8.